

# Determination of Relative Ordering of Activation Energies for Gas-Phase Ion Unimolecular Dissociation by Infrared Radiation for Gaseous Multiphoton Energy Transfer

Michael A. Freitas, Christopher L. Hendrickson, and Alan G. Marshall\*<sup>‡</sup>

Contribution from the Center for Interdisciplinary Magnetic Resonance, National High Magnetic Field Laboratory, Florida State University, 1800 East Paul Dirac Drive, Tallahassee, Florida 32310

Received July 19, 1999

**Abstract:** We report the use of a continuous-wave (CW) CO<sub>2</sub> laser for the determination of relative activation energy for unimolecular dissociation of large biomolecular ions. The [M + 5H]<sup>5+</sup> and [M + 11H]<sup>11+</sup> ions of bovine ubiquitin and the [M + H]<sup>+</sup> ion of bradykinin are irradiated with a CW CO<sub>2</sub> laser and the rate constant for dissociation at each of several laser intensities recorded. A plot of the natural logarithm of the first-order rate constant versus the natural logarithm of laser intensity yields a straight line whose slope provides an approximate measure of the activation energy ( $E_a$ ) for dissociation. For dissociation of protonated bradykinin, the absolute  $E_a$  value from infrared multiphoton dissociation (IRMPD) agrees with that obtained by blackbody infrared radiative dissociation (BIRD), whereas the IRMPD-determined  $E_a$ s for dissociation of the 5+ and 11+ charge states of bovine ubiquitin are lower than those obtained by BIRD. The relative  $E_a$  values for the 5+ and 11+ charge states of bovine ubiquitin from both BIRD and IRMPD are in good agreement. Master equation modeling was carried out on the model peptide, (AlaGly)<sub>8</sub>, to characterize the nature of the internal energy distribution produced from irradiation by a monochromatic IR source (e.g., CW CO<sub>2</sub> laser) versus a broadband IR source (e.g., blackbody). The master equation simulation shows that the internal energy distribution produced by irradiation with the CO<sub>2</sub> laser is essentially identical to that obtained by blackbody irradiation. Our combined experimental and theoretical results justify the IRMPD technique as a viable method for the determination of relative ordering of activation energies for dissociation of large (>50 atoms) ions.

## Introduction

The introduction of electrospray ionization (ESI) has fueled explosive growth in applications of mass spectrometry (MS) to biomolecules.<sup>1–5</sup> ESI-MS has primarily opened up new avenues to probe the solution-phase properties of biomolecules, but has also provided access to aspects of structure, stability, and reactivity of multiply charged gas-phase high-mass (>1000 Da) ions. A primary question is whether biomolecules maintain all or part of their structure upon desolvation to form gas-phase ions. Although there is no direct method to obtain the three-dimensional structure of multiply charged gas-phase high-mass ions, some insight may be gained from gas-phase ion dissociation,<sup>6–11</sup> hydrogen/deuterium (H/D) exchange,<sup>12–19</sup> and ion mobility<sup>20–27</sup> techniques.

A particularly promising class of problems is the binding in noncovalent complexes.<sup>28–33</sup> Solution-phase H/D exchange

offers a means for rapid mapping of the binding sites or interface contact surfaces, whereas gas-phase ion dissociation techniques have the potential to characterize the kinetics and energetics of

\* To whom correspondence should be addressed.  
<sup>‡</sup> Member of the Department of Chemistry, Florida State University, Tallahassee, Florida.  
 (1) Fenn, J. B.; Mann, M.; Meng, C. K.; Wong, S. F.; Whitehouse, C. M. *Science* **1989**, *246*, 64–71.  
 (2) Fenn, J. B.; Mann, M.; Meng, C. K.; Wong, S. F. *Mass Spectrom. Rev.* **1990**, *9*, 37–70.  
 (3) Mann, M.; Meng, C. K.; Fenn, J. B. *Anal. Chem.* **1989**, *61*, 1702–1708.  
 (4) Mann, M. *Org. Mass Spectrom.* **1990**, *25*, 575–587.  
 (5) Whitehouse, C. M.; Dreyer, R. N.; Yamashita, M.; Fenn, J. B. *Anal. Chem.* **1985**, *57*, 675–679.  
 (6) Biemann, K. In *Mass Spectrometry of Biological Materials*; McEwen, C. N., and Larsen, B. S., Eds.; Marcel Dekker: New York, 1990; pp 3–24.  
 (7) Busch, K. L.; Glish, G. L.; McLuckey, S. *Mass Spectrometry/Mass Spectrometry: Techniques and Applications of Tandem Mass Spectrometry*; VCH: Deerfield, FL, 1988.

(8) McLafferty, F. W.; Amster, I. J.; Furlong, J. J. P.; Loo, J. A.; Wang, B. H.; Williams, E. R. In *Fourier Transform Mass Spectrometry: Evolution, Innovation, and Applications*; Buchanan, M. V., Ed.; ACS Symposium Series; American Chemical Society: Washington, D. C., 1987; Vol. 359, pp 116–126.  
 (9) McLafferty, F. W. In *Tandem Mass Spectrometry*; McLafferty, F. W., Ed.; Wiley: New York, 1983.  
 (10) Loo, J. A.; Edmonds, C. G.; Smith, R. D. *Anal. Chem.* **1991**, *63*, 2488–2499.  
 (11) Williams, E. R. *Anal. Chem.* **1998**, *70*, 179A–185A.  
 (12) Griffey, R. H.; Greig, M. J.; Laude, D. A. *Rapid Commun. Mass Spectrom.* **1999**, *13*, 113–117.  
 (13) Heck, A. J. R.; Jorgensen, T. J. D.; O'Sullivan, M.; von Raumer, M.; Derrick, P. J. *J. Am. Soc. Mass Spectrom.* **1998**, *9*, 1255–1266.  
 (14) Wyttenbach, T.; Bowers, M. T. *J. Am. Soc. Mass Spectrom.* **1999**, *10*, 9–14.  
 (15) Green, M. K.; Lebrilla, C. B. *Int. J. Mass Spectrom. Ion Processes* **1998**, *175*, 15–26.  
 (16) Robinson, J. M.; Greig, M. J.; Laude, D. A. *Anal. Chem.* **1998**, *70*, 3566–3571.  
 (17) Freitas, M. A.; Hendrickson, C. L.; Emmett, M. R.; Marshall, A. G. *J. Am. Soc. Mass Spectrom.* **1998**, *9*, 1012–1019.  
 (18) Freitas, M. A.; Shi, S. D.-H.; Hendrickson, C. L.; Marshall, A. G. *J. Am. Chem. Soc.* **1998**, *120*, 10187–10193.  
 (19) Freitas, M. A.; Hendrickson, C. L.; Emmett, M. R.; Marshall, A. G. *Int. J. Mass Spectrom.* **1999**, *185–187*, 565–575.  
 (20) Clemmer, D. E.; Jarrold, M. F. *J. Mass Spectrom.* **1997**, *32*, 577–592.  
 (21) Liu, Y.; Valentine, S. J.; Clemmer, D. E. *Anal. Chem.* **1997**, *69*, 728A–735A.  
 (22) Fye, J. L.; Woenckhaus, J.; Jarrold, M. F. *J. Am. Chem. Soc.* **1998**, *120*, 1237–1328.  
 (23) Shelimov, K. B.; Clemmer, D. E.; Hudgins, R. R.; Jarrold, M. F. *J. Am. Chem. Soc.* **1997**, *119*, 2240–2248.

solvent-free “naked” biomacromolecular complexes. Unimolecular dissociation techniques conducted with trapped ions are best suited to the determination of binding energy in such complexes.<sup>11,34</sup>

Dunbar first showed how absolute value bond dissociation energies of small molecules could be determined by continuous-wave (CW) CO<sub>2</sub> laser irradiation.<sup>35</sup> In particular, for small molecules with few vibrational modes, he showed that, after a short induction period, monochromatic infrared (IR) laser irradiation can closely approximate the effect of steady-state blackbody irradiation, especially if the molecule has a strongly absorbing vibrational mode near the laser frequency.<sup>36</sup> Conversely, a vacuum chamber heated to a specified temperature acts as a blackbody source of IR photons,<sup>37</sup> so that the energy flux entering and leaving an ion population equilibrates with the blackbody, and the internal energy distribution of the ion population is a Boltzmann distribution at the blackbody temperature.

The method of heating ions by blackbody emission to the point of dissociation, initially denoted as zero-pressure thermal radiation—infrared dissociation and later renamed blackbody induced radiative dissociation (BIRD), has been successfully applied to determine bond dissociation energies of clusters<sup>38–45</sup> and biomolecules.<sup>46–57</sup> The principal disadvantage of BIRD is

(24) Shelimov, K. B.; Jarrold, M. F. *J. Am. Chem. Soc.* **1996**, *118*, 10313–10314.

(25) Jarrold, M. F. *Acc. Chem. Res.* **1999**, *32*, 360–367.

(26) Wyttenbach, T.; von Helden, G.; Bowers, M. T. *J. Am. Chem. Soc.* **1996**, *118*, 8355–8364.

(27) Bowers, M. T.; Wyttenbach, T.; Batka, J. J.; Weis, P.; Gidden, J. *Polym. Prepr. (Am. Chem. Soc., Div. Polym. Chem.)* **1997**, *38*, 535–536.

(28) Loo, J. A. *Mass Spectrom. Rev.* **1997**, *16*, 1–23.

(29) Jorgensen, T. J. D.; Roepstorff, P.; Heck, A. J. R. *Anal. Chem.* **1998**, *70*, 4427–4432.

(30) Bruce, J. E.; Smith, V. F.; Liu, C. L.; Randall, L. L.; Smith, R. D. *Protein Sci.* **1998**, *7*, 1180–1185.

(31) Chen, Y.-L.; Campbell, J. M.; Collings, B. A.; Konermann, L.; Douglas, D. J. *Rapid Commun. Mass Spectrom.* **1998**, *12*, 1003–1010.

(32) Veenstra, T. D. *Biochem. Biophys. Res. Commun.* **1999**, *257*, 1–5.

(33) Pramanik, B. N.; Bartner, P. L.; Mirza, U. A.; Liu, Y. H.; Ganguly, A. K. *J. Mass Spectrom.* **1998**, *33*, 911–920.

(34) McLuckey, S. A.; Goeringer, D. E. *J. Mass Spectrom.* **1997**, *35*, 461–474.

(35) Dunbar, R. C. *J. Chem. Phys.* **1991**, *95*, 2537–2548.

(36) Dunbar, R. C.; Zanewski, R. C. *J. Chem. Phys.* **1992**, *96*, 5069–5075.

(37) Dunbar, R. C.; McMahon, T. B. *Science* **1998**, *279*, 194–197.

(38) Dunbar, R. C. *J. Phys. Chem.* **1994**, *98*, 8705–8712.

(39) Dunbar, R. C.; McMahon, T. B.; Tholmann, D.; Tonner, D. S.; Salahub, D. R.; Wei, D. *J. Am. Chem. Soc.* **1995**, *117*, 12819–12825.

(40) Rodriguez-Cruz, S. E.; Jockusch, R. A.; Williams, E. R. *J. Am. Chem. Soc.* **1999**, *121*, 1986–1987.

(41) Rodriguez-Cruz, S. E.; Jockusch, R. A.; Williams, E. R. *J. Am. Chem. Soc.* **1998**, *120*, 5842–5843.

(42) Tholmann, D.; Tonner, D. S.; McMahon, T. B. *J. Phys. Chem.* **1994**, *98*, 2002–2004.

(43) Beyer, M.; Williams, E. R.; Bondybey, V. E. *J. Am. Chem. Soc.* **1999**, *121*, 1565–1573.

(44) Tonner, D. S.; Tholmann, D.; McMahon, T. B. *Chem. Phys. Lett.* **1995**, *233*, 324–330.

(45) Schindler, T.; Berg, C.; Niedner-Schatteburg, G.; Bondybey, V. E. *Chem. Phys. Lett.* **1996**, *250*, 301–308.

(46) Jockusch, R. A.; Schnier, P. D.; Price, W. D.; Strittmatter, E. R.; Demirev, P. A.; Williams, E. R. *Anal. Chem.* **1997**, *69*, 1119–1126.

(47) Price, W. D.; Schnier, P. D.; Williams, E. R. *Anal. Chem.* **1996**, *68*, 859–866.

(48) Price, W. D.; Schnier, P. D.; Jockusch, R. A.; Strittmatter, E. F.; Williams, E. R. *J. Am. Chem. Soc.* **1996**, *118*, 10640–10644.

(49) Schnier, P. D.; Price, W. D.; Jockusch, R. A.; Williams, E. R. *J. Am. Chem. Soc.* **1996**, *118*, 7178–7189.

(50) Jockusch, R. A.; Williams, E. R. *J. Phys. Chem. A* **1998**, *102*, 4543–4550.

(51) Gross, D. S.; Zhao, Y.; Williams, E. R. *J. Am. Soc. Mass Spectrom.* **1997**, *8*, 519–524.

(52) Klassen, J. S.; Schnier, P. D.; Williams, E. R. *J. Am. Soc. Mass Spectrom.* **1998**, *9*, 1117–1124.

that the blackbody source is the vacuum chamber of the Fourier transform—ion cyclotron resonance (FT-ICR) mass spectrometer itself. Changing the temperature requires heating the region of the vacuum chamber surrounding the ions to a uniform temperature and maintaining that temperature throughout the course of the experiment. Temperature reequilibration of the vacuum chamber can take hours. Moreover, BIRD experiments cannot be conducted on thermally labile species, for example, isolation of protein conformational isomers requiring lengthy prior in-trap H/D exchange before BIRD analysis. Finally, it is difficult to heat the vacuum chamber to above 200 °C because of instability or outgassing of components. A heated wire filament<sup>58</sup> and a CW CO<sub>2</sub> laser<sup>59</sup> have thus been offered as alternative IR sources.

Here we extend the original Dunbar approach to determine the dissociation energy of large biomolecular ions.<sup>35</sup> Our source of IR photons is the same CW CO<sub>2</sub> laser used qualitatively by many groups as a standard technique for activating ion dissociation for tandem FT-ICR MS of biomolecules.<sup>60,61</sup> The technique, known as infrared multiphoton dissociation, or IRMPD, is faster than collision-induced dissociation (CID) techniques because the pumping required to remove the neutral collision gas used for CID is not needed, resulting in increased throughput. For our present purposes, a CW CO<sub>2</sub> laser source eliminates the need to maintain a heated vacuum chamber and thus reduces the time required to determine the activation energy,  $E_a$ , for dissociation. We measure unimolecular ion dissociation rate constant,  $k_d$ , as a function of laser intensity.<sup>59</sup> From the slope of a plot of  $\log_e(k_d)$  versus  $\log_e(\text{laser intensity})$ , we determine the experimental activation energy for dissociation of bradykinin as well as bovine ubiquitin, and compare the resultant  $E_a$  values with those previously obtained by BIRD.<sup>59</sup> Finally, we perform master equation modeling (see below) for a simple model peptide, (AlaGly)<sub>8</sub>, to compare the internal energy distribution produced by monochromatic IR irradiation with that from a blackbody.

## Experimental Section

**Instrumentation.** The present experiments were performed with a previously described 9.4 T ESI FT-ICR mass spectrometer configured for external ion accumulation.<sup>63,64</sup> Bovine ubiquitin and bradykinin were infused into a tapered 50  $\mu\text{m}$  i.d. fused silica micro-ESI needle<sup>65,66</sup> at a rate of 300 nL min<sup>-1</sup> at a concentration of  $\sim 10 \mu\text{M}$ . Typical ESI conditions were: needle voltage = 2.5 kV and heated capillary current

(53) Price, W. D.; Schnier, P. D.; Williams, E. R. *J. Phys. Chem.* **1997**, *101*, 664–673.

(54) Price, W. D.; Jockusch, R. A.; Williams, E. R. *J. Am. Chem. Soc.* **1997**, *119*, 11988.

(55) Price, W. D.; Jockusch, R. A.; Williams, E. R. *J. Am. Chem. Soc.* **1998**, *120*, 3474–3484.

(56) Schnier, P. D.; Price, W. D.; Strittmatter, E. F.; Williams, E. R. *J. Am. Soc. Mass Spectrom.* **1997**, *8*, 771–780.

(57) Schnier, P. D.; Williams, E. R. *Anal. Chem.* **1998**, *70*, 3033–3041.

(58) Sena, M.; Riveros, J. M. *J. Phys. Chem. A* **1997**, *101*, 4384–4391.

(59) Freitas, M. A.; Hendrickson, C. L.; Marshall, A. G. *Rapid Commun. Mass Spectrom.* **1999**, *13*, 1639–1642.

(60) Woodlin, R. L.; Bomse, D. S.; Beauchamp, J. L. *J. Am. Chem. Soc.* **1978**, *100*, 3248–3250.

(61) Little, D. P.; Speir, J. P.; Senko, M. W.; O’Connor, P. B.; McLafferty, F. W. *Anal. Chem.* **1994**, *66*, 2809–2815.

(62) Reference deleted in proof.

(63) Senko, M. W.; Hendrickson, C. L.; Emmett, M. R.; Shi, S. D.-H.; Marshall, A. G. *J. Am. Soc. Mass Spectrom.* **1997**, *8*, 970–976.

(64) Senko, M. W.; Hendrickson, C. L.; Pasa-Tolic, L.; Marto, J. A.; White, F. M.; Guan, S.; Marshall, A. G. *Rapid Commun. Mass Spectrom.* **1996**, *10*, 1824–1828.

(65) Emmett, M. R.; White, F. M.; Hendrickson, C. L.; Shi, S. D.-H.; Marshall, A. G. *J. Am. Soc. Mass Spectrom.* **1998**, *9*, 333–340.

(66) Emmett, M. R.; Caprioli, R. M. *J. Am. Soc. Mass Spectrom.* **1994**, *5*, 605–613.

= 3.5 A. Ions accumulated in a linear octopole ion trap (operated at 1.5 MHz) for 1–5 s were transferred through a second octopole ion guide (operated at 1.5 MHz) to a 10-cm-diameter 30-cm-long open-cylindrical Penning ion trap. To each end cap electrode, 2 V was applied to provide a reasonable signal-to-noise ratio while minimizing radial magnetron expansion. The 5+ and 11+ charge states of bovine ubiquitin and the [M + H]<sup>+</sup> ion of bradykinin were individually isolated by SWIFT<sup>67,68</sup> mass-selective ion ejection, and irradiated with a Synrad (Mukilteo, WA; model 48–2) CW CO<sub>2</sub> laser ( $\lambda = 10.6 \mu\text{m}$ ) aligned on-axis with the ion cloud.

The laser beam diameter was taken as the factory-reported value of 3.5 mm. To ensure complete irradiation of the ion cloud throughout the course of the experiment, the laser beam diameter was expanded to ~9 mm by means of a 2.5 $\times$  beam expander (Synrad). Laser beam misalignment results in incomplete dissociation at long irradiation periods, presumably because the ion magnetron radius expands until ions are no longer intercepted by the laser beam. Careful alignment produced linear plots of log<sub>e</sub>(parent ion relative abundance) versus irradiation period, from which unimolecular dissociation rate constants could be determined for each of several laser intensities for the 5+ and 11+ charge states of bovine ubiquitin and for the [M + H]<sup>+</sup> ion of bradykinin. Typical (uncorrected) base pressure for the instrument was  $2 \times 10^{-9}$  Torr, measured by a Granville-Phillips (Boulder, CO) model 274 ion gauge. An Odyssey data station (ThermoQuest, Bremen, Germany) controlled all experiments. Data acquisition was automated by use of a tool command language script.<sup>69</sup> A typical experiment (consisting of eight different irradiation periods for each of five different laser intensities) was completed in ~4 h, or about the same length of time required to equilibrate the vacuum chamber temperature for BIRD determination of a single dissociation rate constant. Each time-domain ICR signal (sum of nine transients) was subjected to baseline correction followed by Hanning apodization<sup>70</sup> and one zero-fill<sup>70</sup> before Fourier transformation and magnitude calculation. The average standard deviation in the parent ion relative abundance was ~5%.

**Sample Preparation.** All samples were obtained from Sigma Chemical Co. (St. Louis, MO) and used without further purification. Samples were initially dissolved in water to give a 1 mM solution. The samples were then diluted in 50:50 (v/v) H<sub>2</sub>O:CH<sub>3</sub>OH to a final concentration of 10  $\mu\text{M}$ . Acetic acid (~5% v/v) was added to a separate aliquot of the bovine ubiquitin solution to generate higher charge states.

**Master Equation Modeling.** Dunbar, McMahan, and co-workers<sup>37–39</sup> and Williams and co-workers<sup>46–49</sup> have investigated extensively the unimolecular dissociation kinetics of low-mass (<1000 Da) ions induced by blackbody irradiation. They firmly established that blackbody emission is responsible for the dissociation of ions at zero pressure.<sup>48</sup> Through the use of master equation modeling, they have shown that a dissociation threshold energy can be extracted from the activation energy obtained by BIRD.<sup>37,48,49,53</sup> For small ions (<50 atoms), master equation modeling is essential to relate the  $E_a$  to the true dissociation threshold,  $E_0$ .<sup>38</sup> For larger ions, the experimentally measured  $E_a$  closely approximates the threshold energy,  $E_0$ .<sup>37</sup> To ascertain whether IRMPD can yield reliable activation energies, we performed master equation modeling of the internal energy distribution of ions irradiated by a CO<sub>2</sub> laser. To establish consistency and reliability for the master equation approach, we compare the internal energy distributions produced by blackbody IR and CW CO<sub>2</sub> laser irradiation of the same model peptide, (AlaGly)<sub>8</sub>, described previously by Price et al.<sup>48</sup> We then calculate the blackbody IR and CW CO<sub>2</sub> laser induced dissociation of (AlaGly)<sub>8</sub>.

A coarse-grained master equation model is designed to describe the time-dependent activation and deactivation for a population of ions. Dunbar et al.<sup>71</sup> and Williams and co-workers<sup>48,53</sup> have described in detail

the application of the coarse-grained master equation model to the unimolecular dissociation of ions. One begins by dividing the overall internal energy distribution into several narrow energy “bins.” Activation (deactivation) of the ion results in the ion moving to a higher (lower) energy bin. Dissociation simply removes ions from the bin in which they resided before dissociation. On the time scale of the IRMPD and BIRD experiments, the pressure in the FT-ICR trapped-ion cell (<10<sup>-8</sup> Torr) closely approximates zero pressure,<sup>53</sup> in the sense that the activation and deactivation of the ion is due primarily to absorption and emission of radiation rather than ion-neutral collisions. Therefore, we consider IR radiation the only source of activation/deactivation.

A coupled set of differential equations describes the effect on ion internal energy distribution of the rates of activation/deactivation ( $k_{i,j}$  is the rate constant for change in ion internal energy from the  $i$ th to the  $j$ th energy bin) and dissociation ( $k_{\text{di}}$  represents the rate constant for disappearance of ions from the  $i$ th energy bin).

$$\frac{dN_i(t)}{dt} = -k_{\text{di}}N_i(t) + \sum_j k_{i,j}N_j(t) \quad (1)$$

in which  $N_i(t)$  is the number of ions in the  $i$ th energy bin after  $t$  seconds of exposure to IR radiation. Equation 1 may be expressed in the form of a “transport matrix,” or J-matrix, containing all of the rate constants for movement of the ion population between the energy bins. The diagonal elements of the J matrix are the rate constants for depletion of the ion population for the respective energy bin and the off-diagonal elements satisfy the constraint of detailed balance. The rates of activation and deactivation are given by eqs 2 and 3. The rate of activation/deactivation is governed by the radiation intensity,  $\rho(h\nu)$ , the Einstein A and B coefficients for spontaneous emission and stimulated absorption/emission, and the microcanonical transition probability,  $P_m^n$ , in which  $n$  is the number of quanta and  $m$  is the frequency mode.

$$K_1(i \rightarrow j) = \sum_{h\nu=\Delta E(i \rightarrow j)} \rho(h\nu)B_{ij}P_m^n \quad (2)$$

$$K_{-1}(j \rightarrow i) = \sum_{h\nu=\Delta E(j \rightarrow i)} (A_{ji} + \rho(h\nu)B_{ji})P_m^{n+1} \quad (3)$$

The microcanonical transition probability is a product of the microcanonical occupation probability and the enhanced transition probability. For a harmonic oscillator with  $n$  quanta of energy in the oscillator, the occupation probability is the ratio of the number of ways the other oscillators can partition the remaining energy in the system to the total number of ways the total energy can be partitioned. The occupation probability is determined by calculating the vibrational density of states (DOS) for the system at energy  $E$  and then calculating the vibrational density of states (DOS') for the system (minus the oscillator containing the  $n$  quanta of energy) at the energy  $E'$  where  $E'$  is the remaining energy left in the system after eliminating the oscillator that contains  $n$  quanta of energy. The DOS'/DOS ratio yields the occupation probability. The occupation probability is then multiplied by the enhanced transition probability,  $m + 1$  for absorption and  $m$  for emission. These factors arise because an absorption is  $m + 1$  times more intense from the  $m$  to  $m + 1$  mode than it is from the  $m = 0$  to  $m = 1$  mode and emission is  $m$  times more intense from the  $m$  to  $m - 1$  mode than it is from the  $m = 1$  to  $m = 0$  mode.

The model assumes the system to be a set of weakly coupled harmonic oscillators, allowing energy to flow freely among the oscillators. Because we do not consider coupling of the oscillators or anharmonicity, the rates of absorption and emission are readily determined from the Einstein A and B coefficients for absorption, stimulated emission, and spontaneous emission (eqs 4 and 5).

$$A = 2.88 \times 10^{-9} \left(\frac{\nu}{c}\right)^2 /_{1,0} \quad (4)$$

The Einstein A coefficient has units of s<sup>-1</sup>,  $\nu$  is in Hz, and the integrated IR absorption intensity for the  $m = 0$  to  $m=1$  transition,  $I_{1,0}$ , is expressed in practical units (cm<sup>-1</sup> L mol<sup>-1</sup>).<sup>72,73</sup> To convert from

(67) Guan, S.; Marshall, A. G. *Int. J. Mass Spectrom. Ion Processes* **1996**, *157/158*, 5–37.

(68) Marshall, A. G.; Wang, T.-C. L.; Ricca, T. L. *J. Am. Chem. Soc.* **1985**, *107*, 7893–7897.

(69) Ousterhout, J. *Tcl and the Tk Toolkit*; Addison-Wesley: Reading, MA, 1994.

(70) Marshall, A. G.; Verdun, F. R. *Fourier Transforms in NMR, Optical, and Mass Spectrometry: A User's Handbook*; Elsevier: Amsterdam, 1990.

(71) Lin, C.-Y.; Dunbar, R. C. *J. Phys. Chem.* **1996**, *100*, 655–659.

the units reported by molecular modeling programs ( $\text{km mol}^{-1}$ ) to IUPAC practical units ( $\text{cm}^{-1} \text{L mol}^{-1}$  defined in terms of base 10 logarithms) we used the conversion factor, 43.4.<sup>72</sup> The Einstein  $B$  coefficient has units of  $\text{cm}^3 \text{Hz s}^{-1} \text{J}^{-1}$  with the frequency  $\nu$  in Hz.  $h$  is Planck's constant (in J s).

$$B = \frac{c^3 A}{9\pi h \nu^3} \quad (5)$$

Furthermore, to calculate the rate constants for activation and deactivation, we need the radiation intensity distribution. For BIRD, the IR source is the heated vacuum chamber, which may be represented by a Planck blackbody energy distribution (eq 6), in which ( $u = h\nu/kT$ ).

$$\rho = \frac{8\pi h \nu^3}{c^3} \frac{1}{e^u - 1} \quad (6)$$

$k$  is Boltzmann's constant ( $\text{J K}^{-1}$ ) and  $T$  is absolute temperature (K). For IRMPD experiments, however, the IR radiation source is a CW  $\text{CO}_2$  laser. We elect to describe the CW  $\text{CO}_2$  laser radiation intensity distribution source as a normalized Gaussian distribution centered at  $943 \text{ cm}^{-1}$  with a full-width at half-maximum (fwhm) of  $10 \text{ cm}^{-1}$  (eq 7). The broad fwhm value satisfies the condition of the master equation model that the ion's vibrational frequency(ies) overlap with the frequency of the laser. The reason for this choice is that the current model cannot easily take into consideration the rotational energy levels of the molecule. Thus, we represent the actual situation, namely, rotationally broadened IR absorption bands and a very monochromatic IR laser, by the computationally much more convenient model of infinitely narrow absorption bands and an arbitrarily broadened IR source, so as to account for activation of vibrational modes near the IR laser frequency.

$$I(\nu) = I(\nu_{\text{laser}}) \frac{e^{-\frac{1}{2} \left( \frac{\nu - \nu_{\text{laser}}}{c\sigma} \right)^2}}{\sigma\sqrt{2\pi}} \quad (7)$$

We calculate the unimolecular rate constants for dissociation by Rice–Ramsperger–Kassel–Marcus (RRKM) theory.<sup>74</sup> For consistency, we use the same parameters as in Price's calculation of blackbody IR radiation-induced dissociation rate constant,  $k_d$ , for  $(\text{AlaGly})_8$ .<sup>48</sup> The vibrational frequencies for  $(\text{AlaGly})_8$  were also determined in the same manner as by Price et al.<sup>48</sup> To generate the vibrational frequency spectrum of  $(\text{AlaGly})_8$ , linear starting geometries for both  $(\text{AlaGly})_4$  and  $(\text{AlaGly})_5$  were optimized and their vibrational frequencies calculated from Hyperchem 5.0 (Gainesville, FL) by use of the Austin Model 1 semiempirical method. Their vibrational frequencies were compared and a unique set of frequencies was generated to estimate the additional frequencies generated from the addition of an AlaGly subunit. This set was added three times to the existing set of frequencies of  $(\text{AlaGly})_5$  to estimate the vibrational spectrum of  $(\text{AlaGly})_8$ . We also calculated the geometries and vibrational frequencies for  $(\text{AlaGly})_6$ ,  $(\text{AlaGly})_8$  (this time without approximations), bradykinin, and angiotensin II. The calculated vibrational frequencies for all of the geometry-optimized species were rounded to the nearest integer  $\text{cm}^{-1}$  value for use in subsequent calculations. The bin width for master equation calculations was set at  $100 \text{ cm}^{-1}$ . A smaller bin size rendered the calculations impractically time-consuming. An upper energy boundary was set to three times the highest average internal energy for the peptide ion to minimize effects of the boundary condition on the internal energy distribution.

## Results and Discussion

**Results of Master Equation Modeling of  $(\text{AlaGly})_8$ .** To interpret the activation energy obtained by use of unimolecular

(72) Dunbar, R. C. *Mass Spectrom. Rev.* **1992**, *11*, 309–339.

(73) Sheshadri, K. S.; Jones, R. N. *Spectrochim. Acta* **1963**, *19*, 1013–1085.

(74) Baer, T.; Mayer, P. M. *J. Am. Soc. Mass Spectrom.* **1997**, *8*, 103–115.

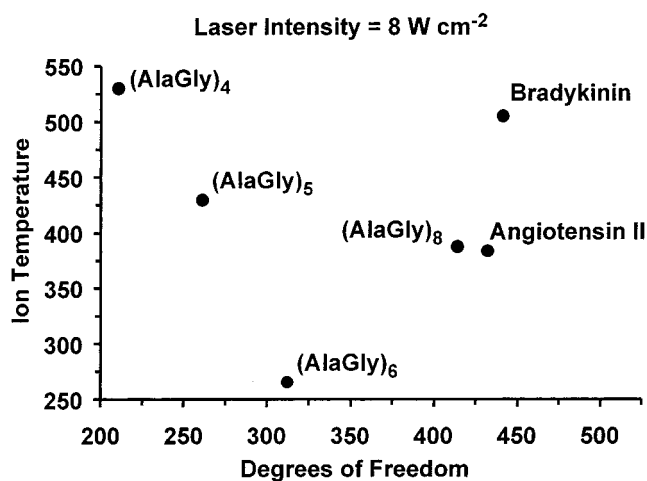


**Figure 1.** Steady-state Boltzmann temperature for each of various protonated peptide cations resulting from irradiation by a CW  $\text{CO}_2$  laser for 3 s at an intensity corresponding to  $4 \text{ W cm}^{-2}$  distributed evenly over a beam of diameter of circular cross-section diameter,  $0.8 \text{ cm}$ .

dissociation methods, we must first understand the internal energy distribution. For simplest interpretation, it is important that the internal energy distribution not become depleted at higher internal energies because of dissociation. Fortunately, Dunbar<sup>38</sup> and Williams and co-workers<sup>48,53</sup> have shown that as the size of a molecule increases, the internal energy distribution becomes less perturbed by ion loss due to dissociation. This effect is due primarily to the increase in the density of states on increase in ion size, for which RRKM theory predicts a decrease in the microcanonical unimolecular dissociation rate constant. In the rapid energy exchange limit (REX),<sup>48</sup> the rates of absorption and emission are much faster than the rate of dissociation. In the REX limit, the ion internal energy maintains a Boltzmann distribution, and a true Arrhenius activation energy can be obtained. Thus, it is important to understand the effect on ion internal energy distribution of irradiation by a monochromatic CW  $\text{CO}_2$  laser.

The master equation model can in principle provide an answer to the question, “do all ions of the same size have the same laser intensity/temperature relation?” If the answer were yes, then there would be no need to calibrate the laser intensity/temperature relation separately for each system of interest. In an attempt to address that question, we calculated the internal energy distributions for  $(\text{AlaGly})_4$ ,  $(\text{AlaGly})_5$ ,  $(\text{AlaGly})_6$ ,  $(\text{AlaGly})_8$ , angiotensin II, and bradykinin during irradiation with a  $\text{CO}_2$  laser at an intensity level of  $8 \text{ W cm}^{-2}$ . From the vibrational frequencies calculated from Hyperchem 5.0, we fitted the internal energy distribution to a Boltzmann distribution. Figure 1 shows the temperature of the internal energy distribution that best fits the internal energy distribution for each of the peptides. It is clear from the data that the internal energy relation to temperature depends strongly on the molecule. Even for the homologous series,  $(\text{AlaGly})_n$ ,  $4 < n < 8$ , the ion temperature at a fixed laser intensity varies nonmonotonically across the series, presumably because of differences in the calculated vibrational frequencies. For example, bradykinin and  $(\text{AlaGly})_4$  each possess a calculated vibration frequency quite close to the laser irradiation frequency, so that they absorb energy more readily than do  $(\text{AlaGly})_n$ ,  $n = 5, 6, 8$ , or angiotensin II. It should be noted that the vibrational frequency spectrum for a single linear conformation of the peptides was performed. A different conformation of the same peptide could produce a different set of frequencies with more/less overlap, resulting in different

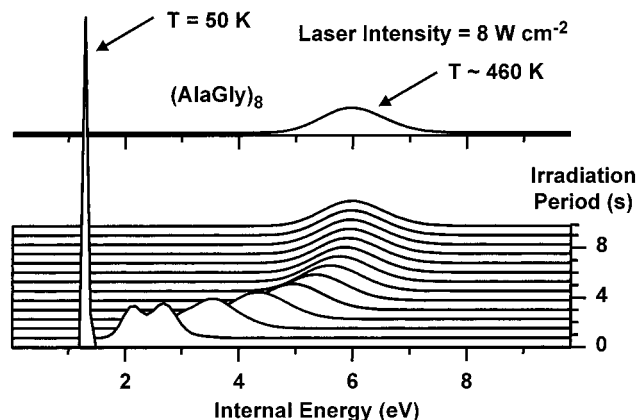


**Figure 2.** Master equation-calculated internal energy distributions for a nondissociating population of (AlaGly)<sub>8</sub> after 1, 2, 3, ..., 10 s of irradiation by a 8 W cm<sup>-2</sup> CW CO<sub>2</sub> laser.

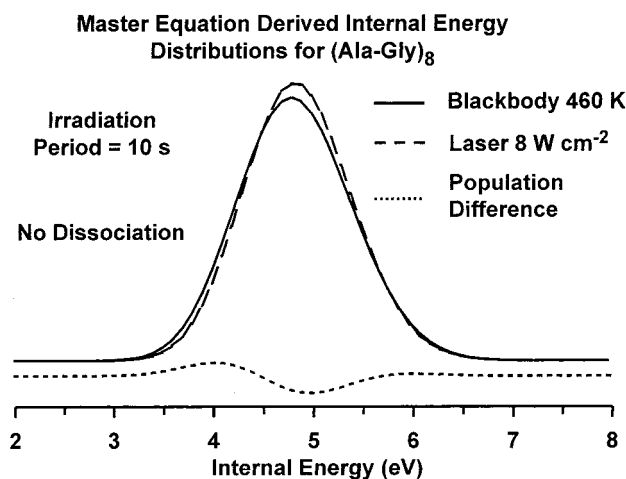


**Figure 3.** Master equation-calculated internal energy distributions for a nondissociating population of (AlaGly)<sub>8</sub> irradiated by either a 460 K blackbody (solid line) or a 8 W cm<sup>-2</sup> CW CO<sub>2</sub> laser (dashed line). The internal energy distribution from 8 W cm<sup>-2</sup> CO<sub>2</sub> laser irradiation very closely resembles that from blackbody IR irradiation.

equilibrium internal energy for the same laser intensity. In fact, the presence of multiple conformations could presumably lead to a distribution of internal energies. In any case, our simple model illustrates that, at this level of theory and molecular size (up to ~1200 Da), the calculated ion temperature at a fixed laser intensity is not constant for different molecules of the same size.

Master equation calculations also reveal the dynamics of IR-induced dissociation. Figure 2 shows the master equation-derived effect of CO<sub>2</sub> IR (wavelength, 10.46 μm; frequency, 943.4 cm<sup>-1</sup>) laser irradiation (8 W cm<sup>-2</sup>) on the internal energy distribution for an initially Boltzmann ( $T = 50$  K) population of (AlaGly)<sub>8</sub>. The internal energy distribution clearly shifts toward higher internal energy during a short (a few seconds) “induction” period, and eventually reaches a steady-state distribution. Curiously, the calculation after 1 s of irradiation produces a transient bimodal distribution that is not fully understood, and that likely arises from imperfect approximations in the model. The main point is that in the absence of ion dissociation, the steady-state internal energy distribution is very well described by a Boltzmann distribution at  $T = 460$  K (see Figure 3). Thus, remarkably, irradiation by a highly monochromatic source quickly leads to a steady-state internal energy distribution that is nearly indistinguishable from that that would result from blackbody heating of the same molecules!

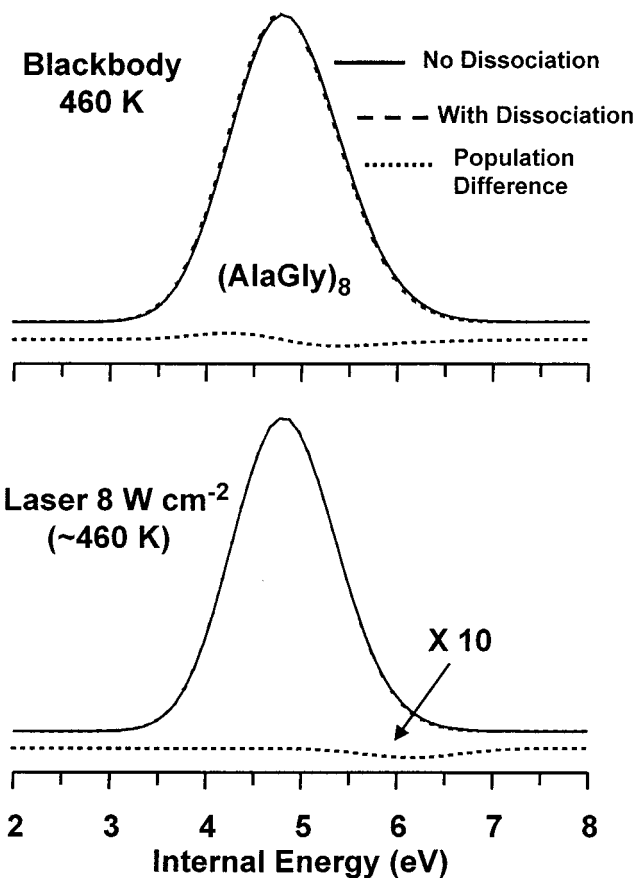


**Figure 4.** Master equation-calculated internal energy distributions for (AlaGly)<sub>8</sub> irradiated by either a 460 K blackbody (top) or a 8 W cm<sup>-2</sup> CW CO<sub>2</sub> laser (bottom), in the absence (solid line) or presence (dashed line) of dissociation, with the difference shown as a dotted line. Note that for both types of irradiation, the distributions in the presence of dissociation are only very slightly perturbed from the distributions in the absence of dissociation.

An equally critical issue is whether the steady-state internal energy distribution maintains its “Boltzmann-like” character when the higher energy population is depleted by dissociation. We therefore first repeated Williams and co-workers’ calculation of the internal energy distribution resulting from blackbody irradiation of (AlaGly)<sub>8</sub> and reproduced their result (Figure 4, top),<sup>48</sup> namely, a very slight change in the internal energy distribution on dissociation (for  $E_0 = 1.52$  eV). Our similar calculation for CO<sub>2</sub> laser irradiation (8 W cm<sup>-2</sup>) of (AlaGly)<sub>8</sub> shows an even smaller change in internal energy distribution when ion dissociation ( $E_0 = 1.52$  eV) is allowed (Figure 4, bottom). Thus, for this peptide model, both blackbody IR and CO<sub>2</sub> laser irradiation produce internal energy distributions that satisfy the REX limit.<sup>48</sup>

**IRMPD-Derived Activation Energy for Dissociation of Protonated Bovine Ubiquitin and Bradykinin Ions.** Activation energies were determined by use of the approximate relation between temperature and laser intensity derived by Dunbar

$$E_a^{\text{laser}} = -\frac{d \ln k_d}{d 1/(kT)} = qh\nu \frac{d \ln k_d}{d \ln I_{\text{laser}}} \quad (8)$$

in which  $q$  is the partition function for the fundamental vibrational mode that absorbs the incoming radiation,  $h$  is Planck’s constant,  $\nu$  is the frequency of the normal mode absorbing the incoming radiation,  $k_d$  is the rate constant for

dissociation, and  $I_{\text{laser}}$  is laser intensity.<sup>35</sup> Over the range of internal energy that we expect to generate (300–500 K), the value for the partition function,  $q$ , for a single vibrational mode at  $943.4 \text{ cm}^{-1}$  will vary between 1.01 and 1.1. Because the internal temperature corresponding to a given laser intensity is not known without calibration, we fix  $q = 1.05$  for all  $E_a$  calculations. Thus, if eq 8 is valid, then the imprecision with which we could measure the activation energy would be  $\sim 10\%$  (5% from uncertainty in  $q$  and 5% from variability of the experimental data). The value for  $E_a$  is then taken as the slope of the line generated by plotting the natural logarithm of the dissociation rate constant versus the natural logarithm of the laser intensity to yield estimates of the activation energies for dissociation of protonated bradykinin and bovine ubiquitin. In fact, eq 8 cannot be used to compare the quantitative behavior of different small molecules, but can still be useful in ordering of activation energies for large molecules.

Dunbar used eq 8 to describe the photodissociation of styrene ions.<sup>35</sup> Although that equation proved correct in predicting the energetics for photodissociation of styrene ions, in which only one vibrational mode was responsible for absorption of incoming radiation, many vibrational modes may absorb at or near the frequency of the laser ( $943.4 \text{ cm}^{-1}$ ) for large molecules. To account for the contribution of multiple modes at or around  $943.4 \text{ cm}^{-1}$ , eq 8 could be multiplied by a scaling factor. Such scaling is necessary for comparison of  $E_a$  values from systems with widely variant vibrational frequencies. However, for a series of molecules with very similar structures and vibrational frequencies, it appears reasonable to assume that the IRMPD-determined  $E_a$  values will also scale similarly. In such a case (i.e., the kind of problem for which the present method is a suggested solution), the resulting  $E_a$  values should provide a reliable ladder of *relative* activation energies.

It is worth noting that the slope of the line used to determine the activation energy in both BIRD [ $\log_e(k_d)$  vs  $1/T$ ] and IRMPD [ $\log_e(k_d)$  vs  $\log_e(I_{\text{laser}})$ ] depends on the range of internal energies of the experiment. As the internal energy increases, the dissociation rate constant falls off because the dissociation rate at higher internal energy becomes competitive with the rates of radiative activation and deactivation. Hence, the population at higher internal energy is rapidly depleted and is not replenished at a sufficient rate to maintain a steady-state distribution. Thus, the rate constant for dissociation depends strongly on the rate of activation of the ion at high internal energy.

Figure 5 is a plot of the relative abundance of protonated bradykinin,  $[M+H]^+$ , as a function of time after  $\text{CO}_2$  laser irradiation ( $30 \text{ W cm}^{-2}$ ). The ion population remains approximately constant during an initial induction period ( $\sim 0.5$  s), during which the ion internal energy distribution evolves to a near-Boltzmann distribution at higher temperature. After the induction period, ion dissociation produces a first-order decrease in parent ion abundance as evidenced by a linear semilog plot. The slope of the line was taken from the first data point after the induction period and the last experimental data point. Figure 6 shows a series of similar plots for protonated bradykinin at each of several laser intensities. The rate of dissociation clearly increases with increasing laser intensity. From the first-order rate constants taken from the slopes of the lines in Figure 6, the activation energy may be obtained from eq 8. Specifically, from the slope of a plot of  $\log_e(k_d)$  versus  $\log_e(I_{\text{laser}})$ , as shown in Figure 7, we obtain an activation energy,  $E_a = 1.17 \pm 0.1$  eV, quite similar to the value (1.25 eV) obtained by Schnier et al. by use of the BIRD technique.<sup>49</sup> The similarity of this result to the BIRD result for the same system suggests that only a

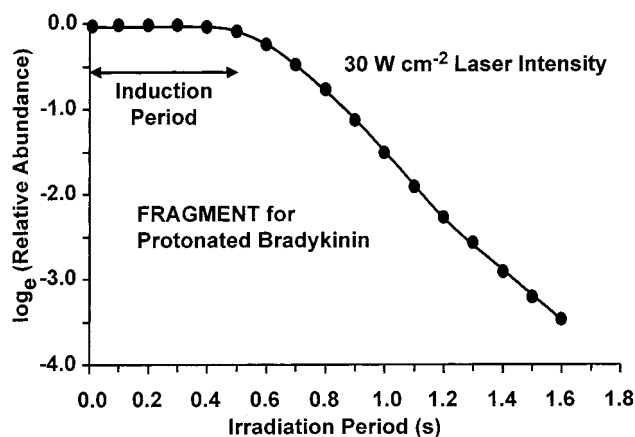


**Figure 5.** Plot of the natural logarithm of parent ion relative abundance versus time for the dissociation of protonated bradykinin during  $30 \text{ W cm}^{-2}$   $\text{CO}_2$  laser irradiation. Note the induction time required before the ions gain sufficiently high internal energy to initiate dissociation, after which first-order decay in population is observed.

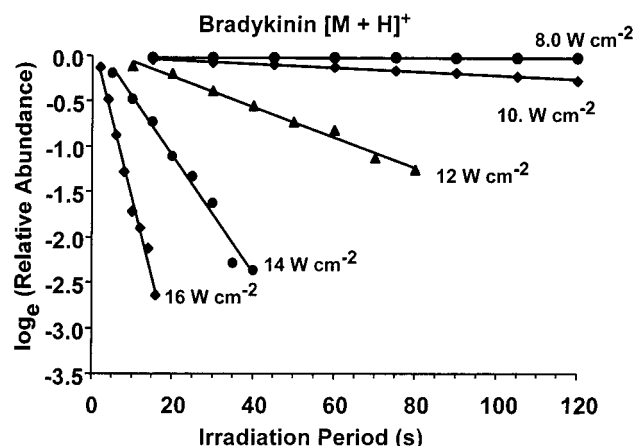


**Figure 6.** Several plots of the type shown in Figure 5, over a longer time scale, for the dissociation of protonated bradykinin at each of several laser intensities.

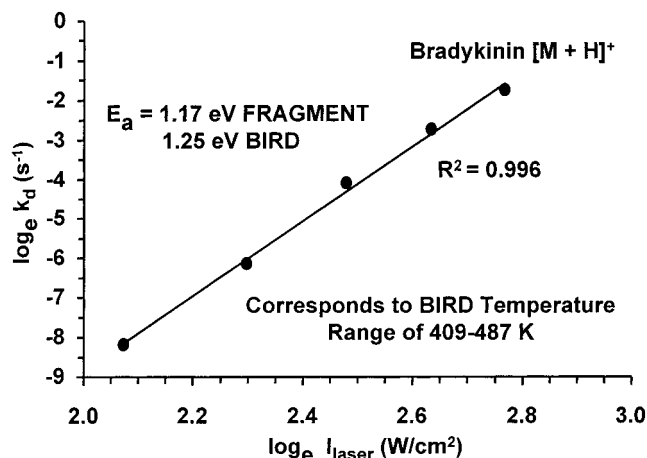


**Figure 7.** Plot of the natural logarithm of the first-order unimolecular dissociation rate constant,  $k_d$ , versus the natural logarithm of laser intensity for protonated bradykinin. The activation energy for dissociation,  $E_a$ , is obtained from the slope of this line (see eq 8). Note the close agreement between the present IRMPD  $E_a$  value and that obtained previously by BIRD.<sup>49</sup>

single mode is responsible for the activation of the bradykinin molecule. The linearity of the data over a wide range of laser intensity further supports the IRMPD technique as a viable alternative to BIRD (see discussion below of Figure 11).

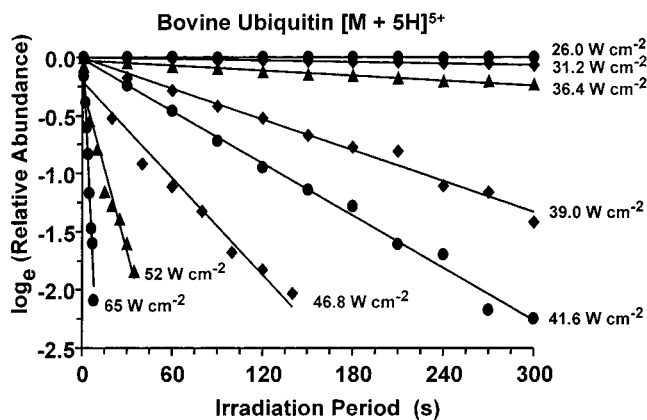


**Figure 8.** Semilog plot of relative abundance of the 11+ charge state of bovine ubiquitin versus period of exposure to CO<sub>2</sub> laser irradiation, for each of several laser intensities. Proceeding from slowest to fastest decay, the laser intensity is 26.0, 31.2, 36.4, 39.0, 41.6, 46.8, 52.0, 65.0 W cm<sup>-2</sup>.

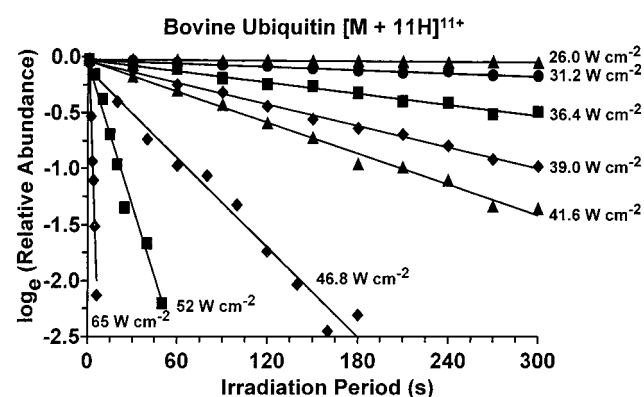


**Figure 9.** Plots as in Figure 8, but for the dissociation of the 11+ charge state of bovine ubiquitin.

We next examine the CO<sub>2</sub> laser-induced dissociation of the protein, bovine ubiquitin. Figures 8 and 9 show the plot of natural logarithm of the protonated parent ion relative abundance versus irradiation period for the 5+ and 11+ charge states of electro sprayed bovine ubiquitin. The activation energies for dissociation of the 5+ and 11+ charge states of bovine ubiquitin were determined as for protonated bradykinin ions: Figure 10 shows plots of  $\log_e(k_d)$  versus  $\log_e(I_{\text{laser}})$  for both the 5+ and the 11+ charge states. The IRMPD-determined activation energy for dissociation of the 5+ (0.7 eV) and 11+ (0.9 eV) charge states significantly underestimates those obtained by BIRD (1.2 and 1.6 eV).<sup>46,48</sup> However, the *ratio* of the activation energies for the two charge states agrees nicely with that from BIRD.

The temperature range of the IRMPD experiment of bovine ubiquitin was calibrated by determining the laser intensity at which the dissociation rate constant is the same as that obtained by a BIRD experiment at the appropriate temperature.<sup>46,48</sup> This comparison provides a means to correlate the IRMPD laser power used to obtain a particular rate of dissociation with the BIRD temperature that would give the same rate. The correlation between laser intensity and temperature was determined by taking a linear regression of a plot of the BIRD rate constant versus  $1/T$ . From that slope and intercept, the temperature that would yield each of the IRMPD rate constants was calculated. Each  $\ln(I_{\text{laser}})$  and its corresponding calculated  $1/T$  value were then plotted in Figure 11. Note the strong correlation for both the 5+ and 11+ charge states in the BIRD temperature range (i.e., the range for the linear regression). Outside the BIRD

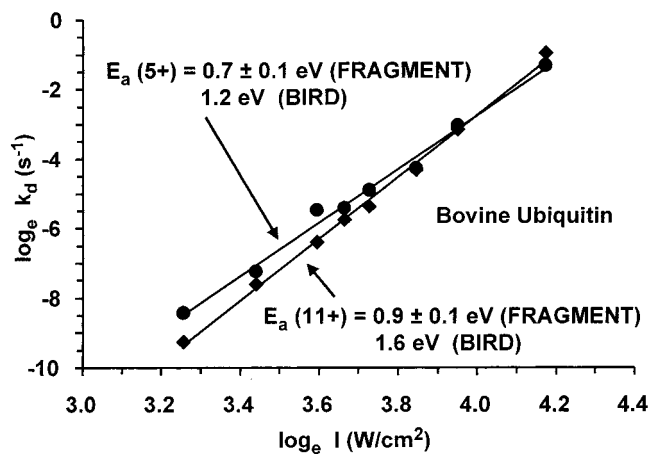


**Figure 10.** Plot of  $\log_e(k_d)$  versus  $\log_e(I_{\text{laser}})$  (as in Figure 7) for the 5+ and 11+ charge states of bovine ubiquitin. Although the *absolute* dissociation activation energies (0.6 and 0.9 eV) determined from the slopes of these lines (see eq 8) are significantly less than those previously obtained from BIRD experiments (1.2 and 1.6 eV),<sup>48</sup> the relative  $E_a$ s for the 5+ and 11+ charge state dissociations are similar to those obtained by BIRD (see text).

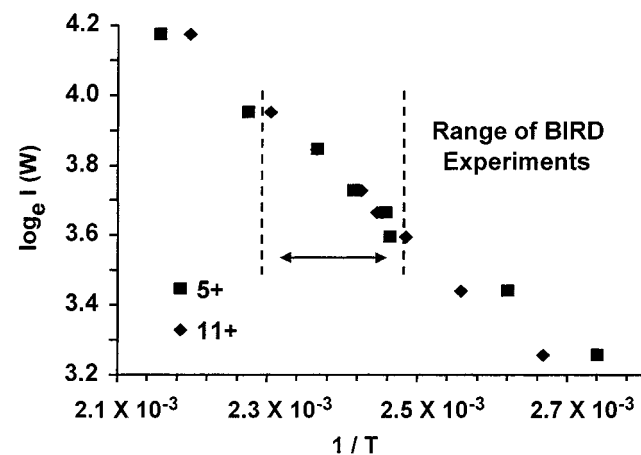


**Figure 11.** Plot of the natural logarithm of laser intensity versus  $1/T$ .  $T$  is determined as the BIRD temperature that yields the same dissociation rate constant as observed for a particular IRMPD laser intensity. The two vertical lines delineate the (much narrower) temperature range of BIRD for the same system.<sup>48</sup>

temperature range, the two lines begin to deviate. However, note that  $\ln(I_{\text{laser}})$  still varies linearly with  $1/T$  for either charge state, as predicted by eq 8. Moreover, Figure 11 shows that the temperature range accessed in the IRMPD experiment is greater than that obtainable by BIRD (Figure 8).

The underestimation of the *absolute* activation energy by IRMPD relative to BIRD for high-mass ions likely follows from the approximation underlying eq 8, namely, that incoming radiation is absorbed by a *single* vibrational mode. As molecular size increases, this assumption may no longer hold. Thus, by scaling the partition function to a value higher than 1.05 [i.e., a way to represent additional vibrational mode(s) at the same frequency] we can improve on the accuracy of *absolute*  $E_a$  obtained from IRMPD experiments. For example, rescaling  $q$  to 1.74 yields  $E_a = 1.2$  and 1.6 eV for the 5+ and 11+ charge states, that is, much better agreement with the BIRD-determined values. Further investigation of the effect of molecular size on the scaling of the partition function is clearly warranted. Finally, even if the scaling factor for  $q$  cannot be determined from BIRD experiments, IRMPD measurements can still yield reliable *relative* activation energies.

### Conclusions and Future Directions

The data presented in this paper demonstrate that IRMPD is a viable technique for the elucidation of *relative ordering* of activation energies for the unimolecular dissociation of protein and peptide ions. CW CO<sub>2</sub> laser irradiation provides a convenient means to control the internal energy of ions without the need to heat the FT-ICR trapped-ion cell or vacuum chamber. Although the temperature/laser intensity relation is not completely understood, the IRMPD technique nevertheless has the potential to provide *relative ordering* of activation energy for a series of ions of similar size and structure. For example, IRMPD could provide a "ladder" of relative activation energies for dissociation of a series of noncovalent adduct ions, such as a series of ligands binding to a common receptor, or a given

ligand binding to a series of site-specifically engineered mutants of a receptor protein. We are currently pursuing such applications.

**Acknowledgment.** We thank John P. Quinn, Daniel McIntosh, and Fei He (National High Magnetic Field Laboratory), Scott McLuckey (Oak Ridge National Laboratory), Robert Dunbar (Case Western Reserve), and William Price (Marshall University) for their technical expertise and helpful discussion. This work was supported by NSF (CHE-93-22824), the NSF National High Field FT-ICR Facility (CHE-94-13008, CHE 99-09502), Florida State University, and the National High Magnetic Field Laboratory in Tallahassee, Florida.

JA9925397